RAPID COMMUNICATIONS

PHYSICAL REVIEW C

NUCLEAR PHYSICS

THIRD SERIES, VOLUME 47, NUMBER 2 FEBRUARY 1993

RAPID COMMUNICATIONS

The Rapid Communications section is intended for the accelerated publication of important new results. Manuscripts submitted to this section are given priority in handling in the editorial office and in production. A Rapid Communication in **Physical Review C** *may be no longer than five printed pages and must be accompanied by an abstract. Page proofs are sent to authors.*

Extraction of the multifragmentation time scale in intermediate energy heavy-ion reactions

D. Fox and R. T. de Souza
Indiana University Cyclotron Facility and Department of Chemistry, Indiana University, Bloomington, Indiana 47405

L. Phair, D. R. Bowman,* N. Carlin,† C. K. Gelbke, W. G. Gong,‡ Y. D. Kim,§ M. A. Lisa, W. G. Lynch, G. F. Peaslee, M. B. Tsang, and F. Zhu**
National Superconducting Cyclotron Laboratory and Department of Physics and Astronomy, Michigan State University, East Lansing, Michigan 48824
(Received 28 September 1992)

The spatial and temporal extent of a system decaying by multifragment emission is deduced. Two-particle intermediate mass fragment correlation functions measured for central $^{36}Ar+^{197}Au$ collisions at $E/A=50$–110 MeV indicate a rapid decay, <75 fm/c, of the highly excited system. Furthermore, the behavior of the correlation function at large relative velocities suggests that considerable charge loss occurs prior to fragment emission.

PACS number(s): 25.70.Pq

Nuclear systems at high excitation can decay by multiple emission of intermediate mass fragments (IMF: $3\leq Z\leq 20$) [1–10]. Key to understanding this phenomenon is knowledge of the source size and lifetime. Both dynamical and statistical theories predict breakup of the system on a relatively short time scale, $\tau\approx 100$ fm/c [3–5,11]. Both theories, however, require a reduction in the nuclear density to correctly predict fragment emission probabilities since fragment formation and emission is substantially enhanced at low density [1,12–14]. Such a reduction in the density of the system might result either from a rapid dynamical compression-decompression cycle induced in central intermediate energy heavy-ion collisions [1–5] or from the thermal pressure of the system [15–18]. At present, however, little experimental information exists about the evolution of the emission time scale and density with increasing excitation [19–21].

To characterize the evolution of the IMF emission time scale with increasing incident energy for central collisions, an excitation function has been measured for the system $^{36}Ar+^{197}Au$ at $E/A=50$, 80, and 110 MeV. The experiment was performed at the National Superconducting Cyclotron Laboratory at Michigan State University (MSU-NSCL). Beams of ^{36}Ar, with an intensity of approximately 1×10^{8} particles per second, impinged on a

*Present address: Chalk River Nuclear Laboratories, Chalk River, Ontario, Canada K0J 1J0.

†Present address: Instituto de Fisica, Universidade de Sao Paulo, C. Postal 20516, CEP 01498, Sao Paulo, Brazil.

‡Present address: Lawrence Berkeley Laboratory, University of California, Berkeley, CA 94720.

§Present address: Indiana University Cyclotron Facility, Indiana University, Bloomington, IN 47405.

**Present address: Brookhaven National Laboratory, Upton, NY 11973.

^{197}Au target of areal density 1 mg/cm^2. Particles emitted in the angular range $9° \leq \theta_{lab} \leq 160°$ were detected with the MSU Miniball array [22]. Each element of the Miniball consists of a 4 mg/cm^2 plastic scintillator foil backed by a 2-cm-thick CsI(Tl) crystal. Particles that punched through the plastic scintillator foils were identified by charge up to $Z=18$. In addition, isotopes of hydrogen and helium were identified. The approximate energy thresholds were $E_{th}/A \approx 2$ MeV for $Z=3$, $E_{th}/A \approx 3$ MeV for $Z=10$, and $E_{th}/A \approx 4$ MeV for $Z=18$. Particles that stopped in the scintillator foil were recorded, but could not be identified by atomic number. Energy calibrations for the forward detectors were obtained by elastic scattering of ^{4}He, ^{6}Li, ^{10}B, ^{12}C, ^{16}O, ^{20}Ne, and ^{35}Cl beams from a ^{197}Au target. The incident energies ranged from $E/A=4.5$ to 20 MeV. For detectors in rings 1–4, $9° \leq \theta_{lab} \leq 40°$, these calibrations are estimated to be accurate to within 5%. During the experiment, the trigger condition required that at least two detectors of the Miniball were triggered in order to record an event.

As shown in Fig. 1(a), intermediate energy, heavy-ion reactions exhibit broad multiplicity distributions. With increasing incident energy the multiplicity distribution extends to larger values of the charged particle multiplicity, N_c, reaching as many as 40 charged particles at $E/A=110$ MeV. A simple geometrical model can be used to relate the charged particle multiplicity N_c to the impact parameter b [23] allowing selection of the same impact parameter range at different bombarding energies. The gates on N_c used to select central collisions are depicted in Fig. 1(a). The gates correspond to $b/b_{max} \leq 0.2$ where the quantity b_{max} corresponds to the maximum impact parameter which will result in events with two charged particles being detected.

The energy spectra of boron fragments from central ^{36}Ar+^{197}Au collisions at $E/A=110$ MeV emitted in the angular range $\theta_{lab}=16°-40°$ are shown in Fig. 1(b). These energy spectra appear to be reasonably described by a single Maxwellian consistent with emission from a single source. The energy spectra of IMFs associated with peripheral collisions, in contrast, are more complex and exhibit a significant nonequilibrium component [24,25]. Thus, restricting the analysis to central collisions might allow comparison of the experimental data to models which stress the equilibrium features of the system formed in central collisions.

The experimental correlation function, $R(v_{red})$, for two IMFs is defined in terms of the ratio of the coincidence yield, Y_{12}, to the product of the single particle yields Y_1 and Y_2:

$$\sum_{p_1,p_2} Y_{12}(p_1,p_2) = C[1+R(v_{red})] \sum_{p_1,p_2} Y_1(p_1)Y_2(p_2)$$

where p_1 and p_2 are the laboratory momenta of IMFs 1 and 2, the reduced velocity is $v_{red}=(p_1/m_1-p_2/m_2)/\sqrt{Z_1+Z_2}$, m_1 and m_2 are the IMF masses, assuming $Z/A=\frac{1}{2}$ for each IMF, and C is a normalization constant determined by the requirement that $\langle R(v_{red})\rangle=0$ at large relative momenta where the final-state interac-

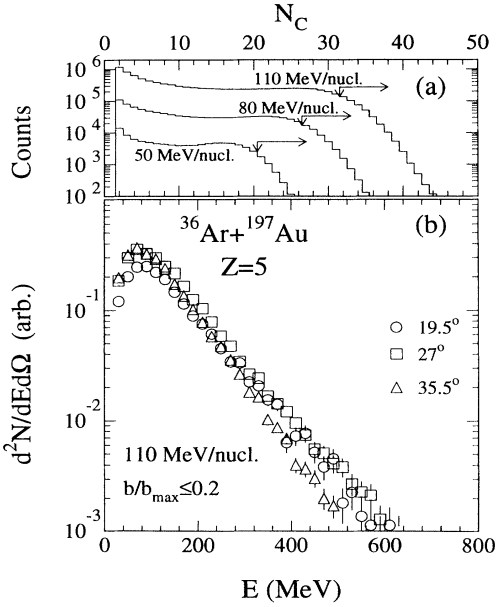

FIG. 1. (a) Charged particle multiplicity, N_c, from ^{36}Ar+^{197}Au reactions at $E/A=50$, 80, and 110 MeV. The arrows indicate gates on N_c used to select central events, $b/b_{max} \leq 0.2$, at each energy based on a simple geometrical model that relates N_c to the impact parameter b. (b) Energy spectra for boron fragments emitted from central events at $E/A=110$ MeV, and $\theta_{lab}=19.5°$ (circles), 27° (squares), and 35.5° (triangles).

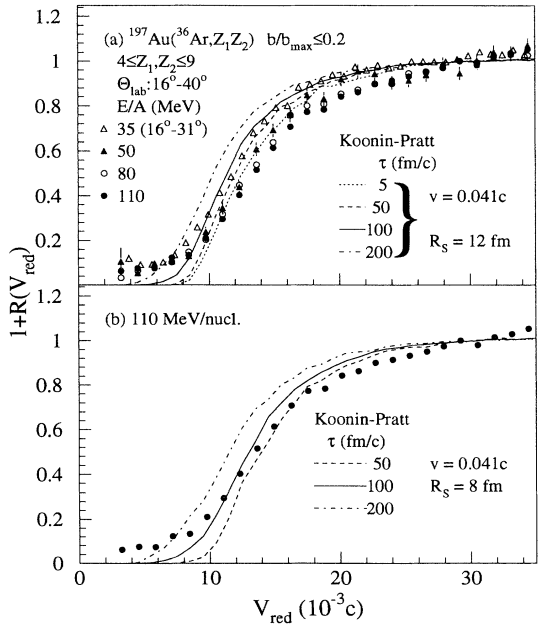

FIG. 2. (a) Two IMF correlation functions for $4 \leq Z_1, Z_2 \leq 9$ emitted at $\theta_{lab}=16°-40°$ for central events from ^{36}Ar+^{197}Au at 50, 80, and 110 MeV/nucleon. Data from Ref. [25] for 35 MeV/nucleon are included for comparison. The results of calculations for the 110 MeV/nucleon data using the Koonin-Pratt formalism are shown as lines, for details see the text. (b) Koonin-Pratt calculations for $R_s=8$ with $v_s=0.041c$ and $\tau=50$, 100, and 200 fm/c.

tion is small. (The use of v_{red}, instead of the relative momentum, allows the correlation functions to be summed over different pairs of IMFs [26].)

The correlation functions for two IMFs emitted in central collisions at the three bombarding energies are shown in Fig. 2(a). The correlation functions are constructed over all IMF pairs with $4 \leq Z_1, Z_2 \leq 9$ emitted into the angular acceptance $16° \leq \theta_{lab} \leq 40°$. Also shown in Fig. 2(a) are data for the same system at 35 MeV/nucleon [26]. At all four beam energies the correlation functions exhibit the same general characteristic of a minimum at small v_{red} arising from the repulsive Coulomb final-state interaction between the two emitted fragments. With increasing incident energy the width of the minimum at small v_{red} becomes larger indicating an increase in the magnitude of the final-state interaction between the emitted IMFs. This increased interaction corresponds to a decrease in the spatial-temporal size of the emitting source.

To extract a mean emission time for the IMFs emitted in central collisions, the experimental correlation functions are compared to theoretical calculations using the Koonin-Pratt formalism [25–27]. The curves shown in Fig. 2(a) correspond to calculations with a mean emission time $\tau = 5$–200 fm/c using the energy spectra associated with central collisions at $E/A = 110$ MeV. Surface emission from a source of radius $R_s = 12$ fm and velocity $v_s = 0.041c$ was assumed. This velocity corresponds to 50% linear momentum transfer at $E/A = 110$ MeV. Using the energy spectra for central events from the other beam energies results in very similar theoretical correlation functions. Comparison of the experimental correlation functions to the theoretical curves reveals that the mean emission time, according to the Koonin-Pratt formalism, decreases from $\tau \approx 100$ fm/c at $E/A = 35$ MeV to $\tau < 50$ fm/c at $E/A = 110$ MeV. These emission times are comparable to the transit time of an Ar projectile past a Au nucleus (80 fm/c at 35 MeV, 50 fm/c at 110 MeV).

Strong final-state interactions, as depicted by the wide Coulomb minima in the data, represent evidence of either a fast emission time scale or a small source size. Disentangling the spatial and temporal extent of the source requires an assumption of the source radius, R_s. The sensitivity of the Koonin-Pratt calculations to the assumption of R_s is shown in Fig. 2(b). If the source radius is assumed to be 8 fm, the data from central interactions at $E/A = 110$ MeV are consistent with $\tau < 75$ fm/c. (For comparison, the radius of a source consisting of two touching carbon nuclei is 5.5 fm.)

Calculations to test the sensitivity of the deduced emission time to the assumption of the source velocity, v_s, were performed. The calculations demonstrated that the deduced mean emission time is fairly insensitive to variations in v_s. In addition, the dependence of the extracted emission time scale on the choice of normalization regions was also explored. For all the data and calculations presented, the normalization constant, C was determined in the region $26 \leq v_{red} \leq 35$. A maximum variation in τ of ≈ 50 fm/c is observed if different regions of v_{red}, $25 \leq v_{red} \leq 45$, are used in determining C.

The presence of a large targetlike residue may affect the IMF correlation functions [19,21,28]. In order to investigate this effect, three-body Coulomb trajectory calculations [25] have been performed. In Fig. 3(a) the results of these calculations for central collisions of $^{36}Ar + ^{197}Au$ at $E/A = 110$ MeV are presented. To provide consistency with our previous two-body Koonin-Pratt calculations the initial source was assumed to be a gold nucleus ($Z_s = 79$, $A_s = 197$) with $R_s = 12$ fm and $v_s = 0.04c$. The calculated correlation function exhibits a much steeper rise at large v_{red} than the data. The rise at large v_{red} can be understood since selection of large v_{red} preferentially selects IMF-IMF pairs with a large opening angle. In these cases, the Coulomb interaction of the heavy residue increases the relative momentum of the IMF pair. In contrast, IMF pairs with small relative momenta preferentially correspond to a small opening angle. In these latter cases, the Coulomb interaction of the heavy residue does not affect the relative velocity. Naturally, a reduction of the atomic number of the emitting source reduces this enhancement of the correlation function at large v_{red}. If the source is assumed to be approximately half the charge of a gold nucleus ($Z_s = 40$ $A_s = 96$, $R_s = 9.4$ fm, $v_s = 0.04$), then the behavior of the experimental correlation function is reproduced at all values of

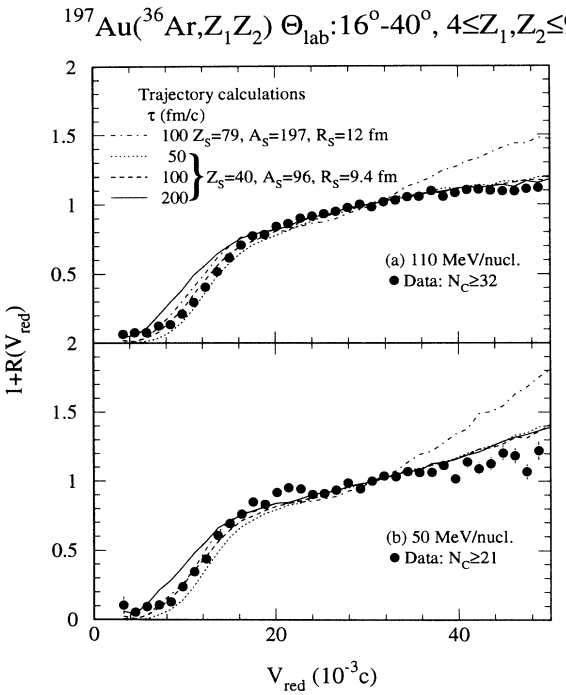

FIG. 3. Results of three-body Coulomb trajectory calculations for central $^{36}Ar + ^{197}Au$ interactions at (a) $E/A = 110$ MeV and (b) $E/A = 50$ MeV. In each panel the data are shown as solid points. The dash-dotted curve is the result of three-body Coulomb trajectory calculations in which the source is a Au nucleus with $R_s = 12$ fm and $v_s = 0.04c$. All other curves represent trajectory calculations for a source with $A_s = 96$, $Z_s = 40$, $R_s = 9.4$, and $v_s = 0.04c$.

v_{red}. The choice of the radius for the $Z_s=40$ nucleus assumes that the density is the same as in the case of the gold nucleus. Comparison of the trajectory calculations with the data also indicate a fast mean emission time, $\tau\approx 75$ fm/c. In Fig. 3(b) the trajectory calculations are compared to the correlation function for central collisions at $E/A=50$ MeV. At this incident energy, the deduced emission time is $\tau\approx 100$ fm/c. The assumption of a large source ($Z_s=79$), in this case, also produces too steep of a rise at large v_{red}, a result inconsistent with the experimental data. Comparison of the experimental data from central collisions at $E/A=80$ MeV with trajectory calculations (not shown) also yield mean IMF emission times of $\tau\approx 100$ fm/c. In all cases, changing R_s, A_s, or v_s only results in a small change in τ, $\Delta\tau<50$ fm/c. Thus, while the behavior of the correlation function at large values of v_{red} exhibits sensitivity to the charge of the emitting system, the shape of the correlation function at small values of v_{red} is dominated by the mean emission time τ.

In summary, two IMF correlation functions have been constructed for central collisions of $^{36}Ar+^{197}Au$ at $E/A=50$, 80, and 110 MeV. Comparison with calculations based on both the Koonin-Pratt two-body formalism and three-body Coulomb trajectory model indicate a short emission time scale, $\tau\approx 50-100$ fm/c, for central events. Furthermore, with increasing incident energy the spatial-temporal size of the emitting system decreases. The deduced emission times are comparable to the transit time of the Ar projectile past the Au target. The extracted emission times are of comparable magnitude to the expansion and equilibration times predicted by microscopic dynamical theories [1]. Statistical models of sequential decays of hot nuclear systems ($T=13$ MeV) also predict comparable emission times ($\tau\approx 80$ fm/c) [11]. However, in such cases the underlying assumption of complete equilibration between successive emissions may not be valid. Coulomb trajectory calculations indicate that the large v_{red} behavior of the correlation function is sensitive to the charge of the emitting source. Based upon these calculations, it appears that substantial charged particle emission occurs prior to multifragment disintegration. Alternatively, the small charge of the emitting system might also be due to fragment formation and emission from the interior of the excited nuclear system particularly at the highest incident energy.

We would like to acknowledge the valuable assistance of the staff and operating personnel of the K1200 cyclotron at the National Superconducting Cyclotron Laboratory for providing the high quality beams which made this experiment possible. This work was supported by the U.S. Department of Energy under DE FG02-92ER40714 and the National Science Foundation under Grants No. PHY-89-13815 and No. PHY-90-15957.

[1] W. Bauer, G. F. Bertsch, and S. Das Gupta, Phys. Rev. Lett. **58**, 863 (1987).
[2] K. Sneppen and L. Vinet, Nucl. Phys. **A480**, 342 (1988).
[3] J. Aichelin, G. Peilert, A. Bohnet, A. Rosenhauer, H. Stocker, and W. Greiner, Phys. Rev. C **37**, 2451 (1988).
[4] G. Peilert, H. Stocker, W. Greiner, A. Rosenhauer, A. Bohnet, and J. Aichelin, Phys. Rev. C **39**, 1402 (1989).
[5] D. H. Boal and J. N. Glosli, Phys. Rev. C **37**, 91 (1988).
[6] L. G. Moretto, Nucl. Phys. **A247**, 211 (1975).
[7] W. A. Friedman and W. G. Lynch, Phys. Rev. C **28**, 16 (1983).
[8] W. A. Friedman and W. G. Lynch, Phys. Rev. C **28**, 950 (1983).
[9] W. A. Friedman, Phys. Rev. C **40**, 2055 (1989).
[10] W. A. Friedman, Phys. Rev. C **42**, 667 (1990).
[11] W. A. Friedman, in *Proceedings of the International Symposium Towards a Unified Picture of Nuclear Dynamics*, Nikko, Japan, 1991, edited by Y. Abe, S. M. Lee, and F. Sakata, AIP Conf. Proc. No. 250 (AIP, New York, 1992), p. 422.
[12] A. Vicentini, G. Jaucci, and V. R. Pandharipande, Phys. Rev. C **31**, 1783 (1985).
[13] R. J. Lenk and V. R. Pandharipande, Phys. Rev. C **34**, 177 (1986).
[14] T. J. Schlagel and V. R. Pandharipande, Phys. Rev. C **36**, 162 (1987).
[15] G. Bertsch and P. J. Siemens, Phys. Lett. **126B**, 9 (1983).
[16] H. Sagawa and G. F. Bertsch, Phys. Lett. **155B**, 11 (1985).
[17] H. Schulz, B. Kampfer, H. W. Barz, G. Ropke, and J. Bondorf, Phys. Lett. **147B**, 17 (1984).
[18] S. Levit and P. Bonche, Nucl. Phys. **A437**, 426 (1984).
[19] R. Trockel, U. Lynen, J. Pochodzalla, W. Trautmann, N. Brummund, E. Eckert, R. Glasow, K. D. Hildenbrand, K. H. Kampert, W. F. Muller, D. Pelte, H. J. Rabe, H. Sann, R. Santo, H. Stelzer, and R. Wada, Phys. Rev. Lett. **59**, 2844 (187).
[20] The mean emission time, τ and the "half-life" for intermediate mass fragment (IMF) emission, $\tau_{IMF\text{-}IMF}$, defined in Ref. [19], are related as $\tau=1.44\tau_{IMF\text{-}IMF}$.
[21] R. Bougault, J. Colin, F. Delaunay, A. Genoux-Lubain, A. Hajfani, C. LeBrun, J. F. Lecolley, M. Louvel, and J. C. Steckmeyer, Phys. Lett. B **232**, 291 (1989).
[22] R. T. de Souza, N. Carlin, Y. D. Kim, J. Ottarson, L. Phair, D. R. Bowman, C. K. Gelbke, W. G. Gong, W. G. Lynch, R. A. Pelak, T. Peterson, G. Poggi, M. B. Tsang, and H. M. Xu, Nucl. Instrum. Methods **A295**, 109 (1990).
[23] C. Cavata, M. Demoulins, J. Gosset, M. C. Lemaire, D. L. Hote, J. Poitou, and O. Valette, Phys. Rev. C **42**, 1760 (1990).
[24] L. Phair, D. R. Bowman, C. K. Gelbke, W. G. Gong, Y. D. Kim, M. A. Lisa, W. G. Lynch, G. F. Peaslee, R. T. de Souza, M. B. Tsang, and F. Zhu, Nucl. Phys. **A548**, 489 (1992).
[25] Y. D. Kim, R. T. de Souza, C. K. Gelbke, W. G. Gong, and S. Pratt, Phys. Rev. C **45**, 387 (1992).
[26] Y. D. Kim, R. T. de Souza, D. R. Bowman, N. Carlin, C. K. Gelbke, W. G. Gong, W. G. Lynch, L. Phair, M. B. Tsang, and F. Zhu, Phys. Rev. C **45**, 338 (1992).
[27] Y. D. Kim, R. T. de Souza, D. R. Bowman, N. Carlin, C. K. Gelbke, W. G. Gong, W. G. Lynch, L. Phair, M. B. Tsang, F. Zhu, and S. Pratt, Phys. Rev. Lett. **67**, 14 (1991).
[28] P. A. DeYoung, M. S. Gordon, Xiu qin Lu, R. L. McGrath, John Alexander, D. M. de Castro Rizzo, and L. C. Vaz, Phys. Rev. C **39**, 128 (1989).